In situ coordination of Fe^{2+} to aromatic diamines intercalated into c-zirconium and c-titanium phosphates: evidence from Mössbauer spectroscopy and thermal studies

Giuseppe Alonzo,[a] Nuccio Bertazzi,[a] Carla Ferragina,[b] Aldo La Ginestra,[c] M. Antonietta Massucci[c] and Pasquale Patrono[b]

[a]*Dipartimento di Chimica Inorganica, Università di Palermo, Via Archirafi 26, 90123 Palermo, Italy*
[b]*IMAI–CNR Area della Ricerca di Roma, PO Box 10, 00016 Monterotondo Stazione, Rome, Italy*
[c]*Dipartimento di Chimica, Università di Roma 'La Sapienza', P.le Aldo Moro 5, 00185 Rome, Italy*

Iron(II) can be exchanged into layered c-$Zr(H_2PO_4)(PO_4)$–diamine and c-$Ti(H_2PO_4)(PO_4)$–diamine composites (diamine = 2,2′-bipyridyl, 1,10-phenanthroline, 2,9-dimethyl-1,10-phenanthroline). Mössbauer spectroscopy indicates that an *in situ* iron–amine coordination occurs in the case of iron–bipyridyl– and iron–phenanthroline–c-zirconium phosphate: Fe^{2+} low-spin trischelates $[Fe(bipy)_3]^{2+}$ and $[Fe(phen)_3]^{2+}$ are formed between the layers of the host; high-spin Fe^{2+} also forms complexes in the interlayer region and the chromophores could be any of the possibilities provided by the formulation $[FeN_xO_{6-x}]$ ($x = 1$–4). Iron(II) partially transforms into iron(III) when the former is not stabilized by the formation of strong complex species. The thermal behaviour of the exchanged compounds has been investigated and correlated with the composition of the materials. X-Ray patterns of some of the new materials are also reported.

There is strong and increasing interest in the production of new porous solids obtained by inserting ions or molecules between the layers of layered materials.[1] Special attention has consequently been paid to clays for their accessibility and potential use in various catalytic processes.[2] In our long and continuous investigations onto the layered phosphates of tetravalent metals, we have made wide use of the well characterized a-zirconium phosphate,[3] c-zirconium and c-titanium phosphates[4] (the a and c compounds have different chemical formulae and layer structures[5,6]) for the preparation of new pillared materials, in which the pillars are first- and second-row transition-metal complexes.[7] The coordination compounds can be inserted as such, *e.g.* $[Cu(phen)_3]^{2+}$, $[Ru(phen)_3]^{2+}$ and $[Ru(bipy)_3]^{2+}$ (phen = 1,10-phenanthroline; bipy = 2.2′-bipyridyl) have been intercalated into a- and c-zirconium phosphates and c-titanium phosphate,[8,9] or formed *in situ*, between a ligand intercalated previously in the interlayer region of the exchangers and a transition-metal ion taken up by the composites *via* an ion-exchange process. We have employed bipyridyl, phenanthroline and 2,9-dimethyl-1,10-phenanthroline as ligands, large aromatic diamines known to form very stable coordination compounds with first- and second-row transition-metal ions.[7] Some Pd^{2+}– and Rh^{3+}–diamine–a-zirconium phosphate materials have been used as catalysts in the oxidative carbonylation of aniline[10] and $CO \rightarrow CO_2$ transformation.[11]

In this paper we report a study on the ability of c-zirconium and c-titanium phosphates to form complex species *in situ* between Fe^{2+} and the aromatic diamines mentioned. This completes a previous investigation on a-zirconium phosphate analogues and Fe^{2+}.[12] Also in this case, Mössbauer spectroscopy has been used to probe the interlayer coordination. The thermal and structural characteristics of all the compounds obtained are described and the results are compared with both those concerning the corresponding materials derived from a-zirconium phosphate[12] and those from a study by Tomita *et al.*[13] on the behaviour of c-zirconium phosphate–phenanthroline or –dimethylphenanthroline intercalation compounds and Fe^{2+}. Note, however, that these authors began with c-zirconium phosphate–diamine intercalation compounds different from ours and the iron uptake was carried out *via* a different procedure, both features leading to different results.

Experimental

Chemicals

$ZrOCl_2 \cdot 8H_2O$, $TiCl_4$, H_3PO_4, $FeSO_4 \cdot 4H_2O$ and all other reagents were obtained from C. Erba RPE (highest purity), except the aromatic diamines 2,2′-bipyridyl (bipy), 1,10-phenanthroline (phen) and 2,9-dimethyl-1,10-phenanthroline (dmp), which were Fluka 'Purissimum'.

Starting materials

The layered ion-exchangers c-$Zr(H_2PO_4)(PO_4) \cdot 2H_2O$ (c-ZrP) and c-$Ti(H_2PO_4)(PO_4) \cdot 2H_2O$ (c-TiP) were prepared, characterized and stored as described previously.[14,15] Their interlayer distances (d_i) were 12.23 and 11.60 Å, respectively. The precursor c-ZrP– or c-TiP–aromatic diamine intercalation compounds were obtained by contacting the pre-swelled ethanolic forms of c-ZrP ($d_i = 16.45$ Å) and c-TiP ($d_i = 15.70$ Å) with 0.1 mol dm^{-3} ethanol–water (1 : 1) solutions of the appropriate diamine. The compounds obtained are listed in Table 1 with their chemical compositions (abbreviations in parentheses) and the interlayer distances. Full details concerning their preparation and X-ray diffraction data are given in ref. 16 and 17, respectively, except for c-$Zr(H_2PO_4)(PO_4)bipy_{0.27} \cdot 1.5H_2O$, which was prepared later by contacting 1 mmol of c-ZrP with 30 ml of a 0.01 mol dm^{-3} bipy solution for 5 days at 43 °C.

Table 1 Amine-intercalated c-zirconium and c-titanium phosphates

material[a]		d_i/Å
c-$Zr(H_2PO_4)(PO_4)phen_{0.45} \cdot 3.0H_2O$	(c-ZrP–$phen_{0.45}$)	18.40
c-$Zr(H_2PO_4)(PO_4)bipy_{0.27} \cdot 1.5H_2O$	(c-ZrP–$bipy_{0.27}$)	14.47
c-$Zr(H_2PO_4)(PO_4)bipy_{0.44} \cdot 0.1H_2O$	(c-ZrP–$bipy_{0.44}$)	14.10
c-$Zr(H_2PO_4)(PO_4)dmp_{0.27} \cdot 2.0H_2O$	(c-ZrP–$dmp_{0.27}$)	16.99
c-$Zr(H_2PO_4)(PO_4)dmp_{0.42} \cdot 2.0H_2O$	(c-ZrP–$dmp_{0.42}$)	19.62
c-$Ti(H_2PO_4)(PO_4)phen_{0.47} \cdot 1.5H_2O$	(c-TiP–$phen_{0.47}$)	17.46
c-$Ti(H_2PO_4)(PO_4)bipy_{0.43} \cdot 0.4H_2O$	(c-TiP–$bipy_{0.43}$)	14.60
c-$Ti(H_2PO_4)(PO_4)dmp_{0.24} \cdot 2.0H_2O$	(c-TiP–$dmp_{0.24}$)	17.87

[a]Moles of diamine and hydration water per mole of exchanger were estimated from TG analyses of samples obtained from three independent preparations of each compound. The error measured on both diamine and water was *ca.* 2%.

The X-ray diffraction data for this material are given in Table 3 later.

Iron(II) uptake

The uptake of Fe^{2+} by the precursors was carried out by a batch procedure. Samples of 1 mmol of amine compound were contacted with portions of a 5 mmol dm^{-3} $FeSO_4$ solution such that $[Fe^{2+}]:[\overline{amine}]=1:3$ or 1:1 (the bar above the metal or amine signifies the solid state: thus $[\overline{amine}]=$[intercalated amine]). The 1:3 molar ratio was chosen in order to favour the formation of trischelate low-spin iron(II)–diamine complex species in the interlayer region, as observed for a-$ZrH_{1.67}[Fe(phen)_3]_{0.16}(PO_4)_2\cdot 2.5H_2O$, derived from a-$Zr(HPO_4)_2\cdot H_2O$ (a-ZrP) intercalated with phen,[8] for which Mössbauer spectroscopy established the formation *in situ* of the iron(II)–phen low-spin trischelate.[12] The 1:1 ratio was also tested to obtain materials with higher iron loadings and to see if 1:1 complex species could be formed in the solids. All the batches were maintained at 45 °C for 7 days. This contact time was sufficient for the various materials to reach maximum Fe^{II} uptake and to accomplish eventually the metal ion–ligand interlayer coordination. The suspensions were then filtered, the supernatant analysed for the iron content and the pH decrease, which is a consequence of the Fe^{2+}/H^+ ion-exchange process of the incoming metal ions with the dihydrogenphosphate groups. The solids were washed with distilled water and air-dried and their amine and water contents were determined by thermogravimetry. X-Ray diffractograms (XRDs) were taken for both wet and dried solids in order to follow the phase changes of iron exchange. Generally XRDs give immediate evidence of the coordination of the metal ion to the ligand between the layers since, in order to better accommodate the complex species formed *in situ*, there is an increase in the interlayer distance (corresponding to the first reflection in the XRD patterns). The coordination process is not excluded if the initial interlayer distance is maintained after metal ion uptake.[7]

The iron–diamine complex formation between the layers of the materials was tested by means of Mössbauer spectroscopy, which also provides information on the oxidation state of the iron exchanged in the solid.

Analyses and physical measurements

A Philips diffractometer was employed to monitor phase changes and eventually confirm that the layered structure was retained. Nickel-filtered Cu-Ka radiation was used, and measurements of 2h were accurate to 0.05°. A Stanton Redcroft simultaneous TG–DTA STA-801 model was used to study the thermal behaviour of the various materials and evaluate their amine and water content (heating rate 5 °C min^{-1}, ignition up to 1100 °C to constant mass, in an air flow). Iron uptake was found by following the concentration changes in the supernatants *via* atomic absorption spectrophotometry, with a GBC 903 instrument. ^{57}Fe Mössbauer spectra were recorded at room temperature (in some cases measurements were also made at −193 °C) by using a constant acceleration spectrometer of standard design, counts being recorded on the 512 channels of a multichannel analyser, and a $^{57}Co/Rh$ source maintained at room temperature, with each absorber consisting of 50 mg cm^{-2} of an unground sample. Spectrometer calibration was effected repeatedly using the magnetic hyperfine interaction of metallic iron at room temperature and all isomer shift values (d) are given with respect to a-Fe at room temperature. The spectra were computer-fitted to Lorentzians by a standard iterative least-squares fit program.

Results and Discussion

Before describing the results of the iron uptake, some structural and thermal characteristics of c-ZrP–$bipy_{0.27}$, the newly prepared intercalation material, will be given (the X-ray diffraction pattern of the compound is reported in Table 3 later). Table 1 shows that c-ZrP–$bipy_{0.27}$ and c-ZrP–$bipy_{0.44}$ have very similar interlayer distances, that of the former being slightly larger. The relatively high hydration of the interlayer region of c-ZrP–$bipy_{0.27}$ (1.5 moles of water per mole of compound) may compensate for the almost double diamine content of the near anhydrous c-ZrP–$bipy_{0.44}$. Different arrangements of bipy in the two compounds must be assumed since they have different thermal behaviours, particularly in the temperature interval (300–600 °C) in which most of the organics are lost. In Fig. 3 and 4 (see later) TG–DTA curves of c-ZrP–$bipy_{0.27}$ and c-ZrP–$bipy_{0.44}$ are reported. Between 300 and 600 °C, c-ZrP–$bipy_{0.27}$ loses bipy with two exothermic steps that accompany the two well differentiated mass losses observable in the TG curve; c-ZrP–$bipy_{0.44}$ shows three exotherms in the DTA curve as if, for the more charged bipy compound, an additional strong interaction (between bipy molecules?) had taken place. As for the diamines intercalated in the layered zirconium and titanium phosphates,[7] the loss of bipy overlaps with the water loss due to the condensation of dihydrogenphosphate to pyrophosphate. Above 600 °C, combustion of the remaining interlayer carbon occurs and the sharp, small exotherm at 1000 °C is due to a phase change to cubic ZrP_2O_7.[18] The other thermal characteristics of c-ZrP–$bipy_{0.27}$, which fall within the general behaviour of these materials, will be illustrated later.

c-ZrP–iron–diamine compounds

The formulation of the five materials obtained from the $[Fe^{2+}]:[\overline{amine}]=1:3$ batches (see Experimental) are listed in Table 2 (numbers **1**–**5**). The abbreviations used in the text are given in parentheses. Apart from compound **4**, c-ZrP–$dmp_{0.20}$–$Fe_{0.09}$, the expected $[\overline{iron}]:[\overline{amine}]=1:3$ molar ratios were obtained in the solids. Compounds **1**–**3** have the same diamine contents as their respective precursors, whereas a

Table 2 Formulation and interlayer distance of iron-exchanged materials derived from c-zirconium phosphate

	material[a]		d_1/Å
1	c-$Zr(H_{1.70}Fe_{0.15}PO_4)(PO_4)phen_{0.45}\cdot 1.5H_2O$	(c-ZrP–$phen_{0.45}$–$Fe_{0.15}$)	20.33
2	c-$Zr(H_{1.82}Fe_{0.09}PO_4)(PO_4)bipy_{0.26}\cdot 1.5H_2O$	(c-ZrP–$bipy_{0.26}$–$Fe_{0.09}$)	16.35
3	c-$Zr(H_{1.74}Fe_{0.13}PO_4)(PO_4)bipy_{0.44}\cdot 2.0H_2O$	(c-ZrP–$bipy_{0.44}$–$Fe_{0.13}$)	18.01
4	c-$Zr(H_{1.82}Fe_{0.09}PO_4)(PO_4)dmp_{0.20}\cdot 1.7H_2O$	(c-ZrP–$dmp_{0.20}$–$Fe_{0.09}$)	16.98
5	c-$Zr(H_{1.74}Fe_{0.13}PO_4)(PO_4)dmp_{0.39}\cdot 2.0H_2O$	(c-ZrP–$dmp_{0.39}$–$Fe_{0.13}$)	17.31
6	c-$Zr(H_{1.18}Fe_{0.41}PO_4)(PO_4)phen_{0.45}\cdot 1.8H_2O$	(c-ZrP–$phen_{0.45}$–$Fe_{0.41}$)	18.01
7	c-$Zr(H_{1.50}Fe_{0.25}PO_4)(PO_4)bipy_{0.21}\cdot 1.9H_2O$	(c-ZrP–$bipy_{0.21}$–$Fe_{0.25}$)	am.[b]
8	c-$Zr(H_{1.24}Fe_{0.38}PO_4)(PO_4)bipy_{0.44}\cdot 2.5H_2O$	(c-ZrP–$bipy_{0.44}$–$Fe_{0.38}$)	am.[b]
9	c-$Zr(H_{1.46}Fe_{0.27}PO_4)(PO_4)dmp_{0.10}\cdot 1.9H_2O$	(c-ZrP–$dmp_{0.10}$–$Fe_{0.27}$)	am.[b]
10	c-$Zr(H_{1.52}Fe_{0.24}PO_4)(PO_4)dmp_{0.38}\cdot 2.0H_2O$	(c-ZrP–$dmp_{0.38}$–$Fe_{0.24}$)	17.66

[a]In these formulations the unexchanged protons have been calculated as if all iron was divalent although Mössbauer spectra account for the presence of Fe^{3+} in some materials. [b]am. = amorphous material.

certain elution of ligand occurs during iron uptake for compound **4**. All of the materials remain layered, with a good degree of crystallinity and their XRD patterns show sharp and intense peaks at low 2h values, those corresponding to the interlayer distance. Compounds **1**–**3** undergo expansion on uptake of Fe^{2+}, and the maximum increment of the interlayer distance is given by c-ZrP–bipy$_{0.44}$–Fe$_{0.13}$ (see Table 2). For the dmp–iron derivatives, an interlayer contraction occurs in the case of c-ZrP–dmp$_{0.39}$–Fe$_{0.13}$ (compound **5**), whereas for c-ZrP–dmp$_{0.20}$–Fe$_{0.09}$ (compound **4**) d_{id} remains unchanged. Table 3 shows the X-ray diffraction data for c-ZrP–phen$_{0.45}$–Fe$_{0.15}$, c-ZrP–bipy$_{0.44}$–Fe$_{0.13}$ and c-ZrP–dmp$_{0.39}$–Fe$_{0.13}$.

The formulation of the materials obtained from the $[Fe^{2+}]$:$[\overline{amine}]=1:1$ batches are also reported in Table 2 (numbers **6**–**10**). Compounds **6** and **10** maintain a very good degree of crystallinity and their interlayer distances are practically unchanged with respect to the precursors. Compounds **7**–**9** become markedly amorphous, even though low-intensity broad peaks at low 2h, corresponding to the interlayer distances, are present in the respective XRD patterns.

Considering only the layered materials, compounds **1**–**3** and **6** are deep red–purple, which is the colour of the $[Fe(phen)_3]^{2+}$ and $[Fe(bipy)_3]^{2+}$ coordination compounds and, as will be shown, the Mössbauer results confirm the presence of Fe^{II} low-spin complex species. Compounds **4**, **5** and **10** are white–grey. Taking into account that the iron–dmp complexes are yellow, coordination compounds are probably not formed in the interlayer region, as is also suggested by the Mössbauer data.

In most cases, iron uptake causes a partial elution of the intercalated amines from the solids. The occurrence of this process after exchange is easy to account for. In previous investigations it has been demonstrated that phen, bipy and dmp interact with the a-ZrP or c-ZrP hosts through the protonation of, on average, one nitrogen per diamine with the hydrogenphosphate or dihydrogenphosphate groups of the exchangers.[19,20] When the metal ions enter the layers of the diamine intercalation compound, they can either exchange with protons of the phosphate groups that have not interacted with the amine, and thus be accommodated without disturbing the amine, or cause nitrogen deprotonation to carry out the Fe^{2+}/H^+ ion-exchange process, particularly if the amount of metal in the solid reaches significant levels. In both cases, the coordination of the ligand to the metal ion can occur totally,[12,21,22] partially[12,23–25] or not at all[12,26] and in these two latter possibilities the ligand molecules, no longer anchored to the host, will be eluted from the solid into the contact solution. No elution of ligand ensues when pure bipy–, phen– or dmp–c-ZrP are contacted with 10^{-2} mol dm^{-3} HCl solution.[16] Furthermore, the coordination compounds formed in the constrained space of the interlayer region do not, generally, reach the metal/ligand molar ratios of the corresponding compounds freely obtainable in solution: moieties with $[MN_4O_2]$ and $[MN_2O_4]$ formulations (M = exchanged metal ions) are the most frequently observed; the low-spin $[Fe(phen)_3]^{2+}$ complex species formed in a-ZrP–phen$_{0.48}$ is unique.[12]

c-TiP–iron–diamine compounds

Exchange between Fe^{2+} ions and the three diamine materials (see Table 1) is completely different from that occurring in the c-ZrP analogues. The batches $[Fe^{2+}]$:$[\overline{diamine}]=1:3$ and 1 : 1 yield correspondingly charged materials only for the dmp precursor. In Table 4 are given the chemical formulations of the compounds obtained, with their abbreviations and interlayer distances (numbers **11**–**14**). The d_i values of the compounds that retain a layered structure remain practically unchanged with respect to those of the precursors, and there is only a small contraction for compound c-TiP–dmp$_{0.10}$–Fe$_{0.09}$ (compound **13**) even though *ca.* 60% of the dmp present initially in the solid is eluted.

The $[\overline{Fe}]$:$[\overline{amine}]=1:3$ molar ratio in the solid can be realized only with c-TiP–bipy$_{0.43}$ and both experimental

Table 3 X-Ray diffraction data for c-ZrP–bipy$_{0.27}$ and some iron-exchanged c-ZrP–diamine intercalation compounds

c-ZrP–bipy$_{0.27}$		c-ZrP–phen$_{0.45}$–Fe$_{0.15}$		c-ZrP–bipy$_{0.44}$–Fe$_{0.13}$		c-ZrP–dmp$_{0.39}$–Fe$_{0.13}$	
d/Å	I/I_0[a]	d/Å	I/I_0[a]	d/Å	I/I_0[a]	d/Å	I/I_0[a]
14.47	100	20.33	100	18.01	100	17.31	100
6.60	3	10.15	37	9.05	10	8.58	8
6.14	12	6.33	9	6.50	8	5.98	13
5.90	4	5.46	10	5.69	9	5.69	5
5.27	2	5.02	3	4.35	14	4.24	19
5.03	6	4.76	6	3.89	10	4.16	9
4.79	3	4.49	8	3.83	18	4.06	18
4.66	2	3.93	47	3.70	8	3.64	15
4.00	35	3.44	11	3.31	28	3.57	8
3.88	47	3.33	18	3.23	10	3.49	12
3.31	55	3.27	10	3.13	8	3.31	10
3.27	29	3.15	3	3.01	4	3.25	62
3.23	32	3.03	11	2.67	8	3.07	9
2.90	6	3.01	3	2.58	6	2.68	12
2.68	16	2.86	7			2.65	15
2.65	3	2.75	10				10
		2.68	3				
		2.65	2				

[a]Relative intensity.

Table 4 Formulation and interlayer distances of iron-exchanged materials derived from c-titanium phosphate

	material[a]		d_i/Å
11	c-Ti($H_{1.90}Fe_{0.05}PO_4$)(PO_4)phen$_{0.44}$·1.5H_2O	(c-TiP–phen$_{0.44}$–Fe$_{0.05}$)	17.45
12	c-Ti($H_{1.80}Fe_{0.10}PO_4$)(PO_4)bipy$_{0.30}$·1.3H_2O	(c-TiP–bipy$_{0.30}$–Fe$_{0.10}$)	14.60
13	c-Ti($H_{1.82}Fe_{0.09}PO_4$)(PO_4)dmp$_{0.10}$·3.0H_2O	(c-TiP–dmp$_{0.10}$–Fe$_{0.09}$)	17.14
14	c-Ti($H_{1.52}Fe_{0.24}PO_4$)(PO_4)dmp$_{<0.05}$·3.0H_2O	(c-TiP–dmp$_{<0.05}$–Fe$_{0.13}$)	am.[b]

[a]In these formulations the unexchanged protons have been calculated as if all iron was divalent although Mössbauer spectra account for the presence of Fe^{3+} in some materials. [b]am. = amorphous material.

batches give materials with the same chemical composition, c–TiP–bipy$_{0.30}$–Fe$_{0.10}$. The XRD pattern of the exchanged compound is identical to that of the precursor in shape and position (2h angles) of all the peaks; only the intensities are slightly lower. c-TiP–bipy$_{0.30}$–Fe$_{0.10}$ is pink in contrast to the purple–red c-ZrP analogues, and this, in the absence of Mössbauer results supporting the formation of iron–bipy trischelate (see later), suggests that the complex species is probably formed only on the surface and/or just between the outermost layers of the intercalation compound. Compound c-TiP–phen$_{0.47}$ does not take up more than 0.05 moles of Fe per mole of compound, whatever the experimental conditions. As a consequence, the XRD pattern of the material is completely superimposable, also regarding peak intensities as well, on that of the precursor.[17] Furthermore, taking into account the Mössbauer results, the pale orange colour of c-TiP–phen$_{0.47}$–Fe$_{0.05}$ may be due to trivalent iron.

Unlike the c-ZrP analogues, c-TiP–bipy$_{0.43}$ and c-TiP–phen$_{0.47}$ exhibit a certain difficulty in exchanging iron ions. These two intercalation compounds have been tested in ion-exchange processes with other transition-metal ions such as Co^{II}, Ni^{II} and Cu^{II} and the maximum uptake found was 0.2–0.25 moles of metal ion per mole of intercalation compound.[17] It has been demonstrated recently, by means of FTIR spectroscopy, supported with UV experiments,[27] that bipy and phen are present in a diprotonated form in c-TiP instead of the monoprotonated form as in c-ZrP.[20] The strong interaction of the diamines with the dihydrogenphosphate groups of the host and the fact that Fe^{II} is generally surrounded by a large number of water molecules thus making the approach to the exchanging sites more difficult, could explain the low Fe^{2+}/H^{+} exchange and, consequently, the absence of *in situ* coordination.

In contrast, c-TiP–dmp$_{0.24}$ exchanges Fe^{2+} with great ease. At the same time, the ligand is 'expelled' from the solid so that the material prepared from the 1:1 batch contains very little dmp, since we have formulated the resulting material as c-TiP–dmp$_{<0.05}$–Fe$_{0.24}$. The XRD patterns of the iron-exchanged solids are affected by the dmp elution: c-TiP–dmp$_{<0.05}$–Fe$_{0.24}$ is essentially amorphous and the c-TiP–dmp$_{0.10}$–Fe$_{0.09}$, obtained from the 1:3 batch, shows a relatively intense first peak ($d_i = 17.14$ Å), but no other subsequent reflections are observed.

Mössbauer results

As for the a-ZrP analogues,[12] Mössbauer spectroscopy was used to probe whether in c-ZrP–diamine–iron compounds the metal ion is coordinated to the intercalated amine or merely exchanged into the interlayer region. Table 5 gives the ^{57}Fe Mössbauer parameters of some of the compounds in Table 2.

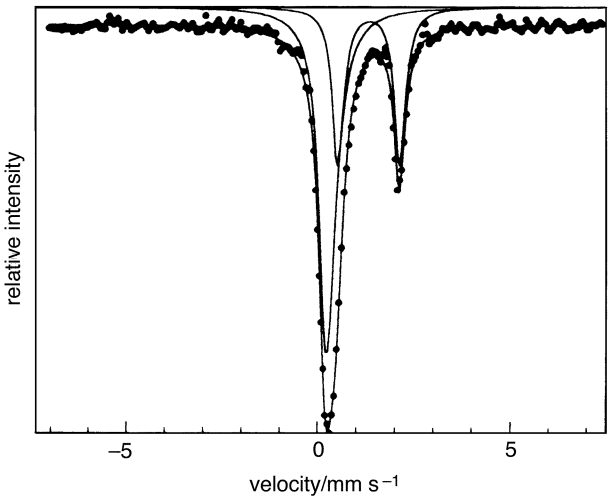

Fig. 1 Room-temperature Mössbauer spectrum of c-ZrP–bipy$_{0.26}$–Fe$_{0.09}$ (compound 2 of Table 2)

The materials obtained from the c-ZrP–phen or –bipy precursors will be considered first. Compounds **1** and **3** give spectra consisting of a single absorption with d and quadrupole splitting (DE) values typical of Fe^{II} low-spin species, which can be identified as $[Fe(phen)_3]^{2+}$ and $[Fe(bipy)_3]^{2+}$, respectively. These results show that, under appropriate stoichiometric conditions, full complexation of Fe^{2+} may indeed occur between the layers of the c-ZrP–diamine precursors. On the other hand, the Mössbauer spectrum of compound **2**, which derives from the new intercalate c-ZrP–bipy$_{0.27}$, shows (Fig. 1) that, as well as a low-spin Fe^{2+} species, *i.e.* $[Fe(bipy)_3]^{2+}$, an appreciable fraction of iron is present as high-spin Fe^{2+} in spite of an iron/diamine molar ratio in the solid appropriate for the complete formation of the trischelate. Not unexpectedly, the Mössbauer spectra of compounds **6**–**8**, with iron/diamine molar ratios appreciably higher than 1/3 (they come from '1:1' batches), contain the characteristic Fe^{2+} quadrupole doublet. In two cases, c-ZrP–phen$_{0.45}$–Fe$_{0.41}$ and c-ZrP–bipy$_{0.21}$–Fe$_{0.25}$ (compounds **6** and **7**), part of the iron is found as the low-spin Fe^{II}–phen or –bipy trischelate complex and part as high-spin Fe^{2+}. For compound **8**, c-ZrP–bipy$_{0.44}$–Fe$_{0.38}$, the deconvol-

Table 5 ^{57}Fe Mossbauer parameters for c-ZrP– and c-TiP–diamine–iron phases at room temperature

		low-spin Fe^{II}				high-spin Fe^{II}				high-spin Fe^{III}			
	material[a]	d[b]	DE[c]	C[d]	I[e]	d[b]	DE[c]	C[d]	I[e]	d[b]	DE[c]	c[d]	I[e]
1	c-ZrP–phen$_{0.45}$–Fe$_{0.15}$	0.30	—[f]	0.47	100								
2	c-ZrP–bipy$_{0.26}$–Fe$_{0.09}$	0.28	—[f]	0.42	62	1.33	1.60	0.34	38				
2	c-ZrP–bipy$_{0.26}$–Fe$_{0.09}$[g]	0.38	—[f]	0.83	23	1.40	3.00	0.40	77				
3	c-ZrP–bipy$_{0.44}$–Fe$_{0.13}$	0.34	0.30	0.41	100								
4	c-ZrP–dmp$_{0.20}$–Fe$_{0.09}$					0.93	2.41	0.30	6	0.48	0.66	0.68	86
						1.04	3.03	0.30	8				
5	c-ZrP–dmp$_{0.39}$–Fe$_{0.13}$					1.07	2.95	0.31	41	0.44	0.71	0.65	59
6	c-ZrP–phen$_{0.45}$–Fe$_{0.41}$	0.27	—[f]	1.00	60	1.12	2.32	0.51	40				
6	c-ZrP–phen$_{0.45}$–Fe$_{0.41}$[g]	0.36	—[f]	1.09	61	1.16	2.93	0.78	39				
7	c-ZrP–bipy$_{0.21}$–Fe$_{0.25}$	0.28	—[f]	0.50	46	1.32	1.66	0.38	54				
7	c-ZrP–bipy$_{0.21}$–Fe$_{0.25}$[g]	0.40	—[f]	0.80	67	1.37	3.03	0.40	33				
8	c-ZrP–bipy$_{0.44}$–Fe$_{0.36}$					1.13	2.00	0.44	13	0.41	0.63	0.80	87
9	c-ZrP–dmp$_{0.10}$–Fe$_{0.27}$					1.08	2.35	0.41	17	0.58	0.62	0.65	83
11	c-TiP–phen$_{0.44}$–Fe$_{0.05}$									0.45	0.84	1.00	100
12	c-TiP–bipy$_{0.30}$–Fe$_{0.10}$					1.26	2.78	0.46	39	0.41	0.84	1.00	61
13	c-TiP–dmp$_{0.10}$–Fe$_{0.09}$					1.25	2.76	0.60	30	0.41	0.72	0.82	70

[a]Numbering as for Tables 2 and 3. [b]Isomer shift (mm s^{-1}) relative to room temperature metallic a-Fe. [c]Quadrupole splitting (mm s^{-1}). [d]FWHM (mm s^{-1}). [e]Subspectrum relative area (%). [f]Fitted to a single Lorentzian. [g]At liquid-nitrogen temperature.

ution of the spectrum is not compatible with any significant contribution from a low-spin Fe^{II} component at $d \# 0.34$ mm s^{-1}, the low-velocity line of the Fe^{2+} doublet being superimposed on an intense, partially resolved, doublet which is assigned to iron(III) species supported by its d value ($\geqslant 0.40$ mm s^{-1}).

Phenomenologically, the large variety of spectral parameter values found for high-spin Fe^{2+} in compounds **2** and **6**–**8** (also the results obtained for the c-ZrP–dmp–iron and c-TiP–diamine–iron phases), is presumably due to different chemical environments of iron in the interlayer, whose precise identification does not appear possible in the majority of the cases. Since the d values are in the range expected for six-coordinate species, the interlayer iron chromophores could correspond to any of the possibilities provided by the formulation FeN_xO_{6-x} ($x = 1$–4) with oxygen coordination to iron considered as coming from interlayer water molecules or skeletal phosphate groups, where the diamine could act as aniso-bidentate (or monodentate for odd x values, where appropriate). Each possibility, *i.e.* each chemical identity, will present its own distorted geometry and hence its own spectral parameters. More precisely, since the d values for high-spin iron(II) species generally increase (the s-electron density at the Mössbauer nucleus decreases) with increasing coordination number and ligand electronegativity, we consequently favour the hypothesis that assigns the highest high-spin Fe^{II} d values shown by compounds **2** and **7** (1.33 and 1.32 mm s^{-1}, respectively, at room temperature) to an FeO_6-type chromophore, the lower d value at *ca.* 1.10 mm s^{-1} being associated with oxygen–diamine containing species. Indeed, the reported d values for the $Fe(H_2O)_6^{2+}$ cation in crystalline $Fe(ClO_4)_2 \cdot 6H_2O$ and $Fe(BF_4)_2 \cdot 6H_2O$ are in the range 1.28–1.34 mm s^{-1},[28–31] (data from ref. 29 and 30 were taken from d *vs.* temperature plots, and converted to our a-Fe zero) so that the species present in compounds **2** and **7** are probably similar to the aquo cation. The spectra of compounds **2** and **7** obtained at -193 °C reveal a further possible analogy with the iron(II) salts mentioned above. Both the perchlorate and tetrafluoborate are examples of high-spin iron(II) salts, which exhibit a considerable jump of DE (from *ca.* 1.3 to *ca.* 3.4 mm s^{-1}) when the temperature changes from room temperature to -193 °C. The strong variation of DE can be associated (electronically) to a degenerate (small DE)/single (large DE) orbital ground-state inversion and could occur (sterically) in either trigonally or tetragonally distorted octahedral symmetry for a change from an elongated to a compressed shape.[29–31] Although smaller, the DE variation observed in our compounds (from *ca.* 1.6 to *ca.* 3.0 mm s^{-1}) seems large enough to be of the same origin as in those salts, while the less important change in DE could derive from different distortion factors for either elongation and compression.

The presence of uncomplexed iron and free bipy together with Fe^{II} low-spin trisbipy complex species in the interlayer region of compound **2**, unlike compound **3** where Fe^{2+} and bipy are completely linked in the low-spin trischelate complex formation, is probably related to the different amounts of bipy in the two compounds and hence to different arrangements of the diamine units in the corresponding precursors c-ZrP–$bipy_{0.27}$ and c-ZrP–$bipy_{0.44}$ (these compounds also show different thermal behaviour, see later). It can be supposed that in c-ZrP–$bipy_{0.27}$ the bipy, because of its lower content, can interact more tightly with its host than in c-ZrP–$bipy_{0.44}$. Thus, the incomplete formation of trischelate species in the interlayer region of the solid, notwithstanding the correct 1 : 3 Fe/bipy molar ratio, may be the result of a compromise between the strength with which the amine interacts with the host and that of coordination to the metal ions. Furthermore, the same d_i value of compound **2**, which is smaller than that of compound **3**, could derive from the strain imposed on the interlayer $[Fe(bipy)_3]^{2+}$ units formed by the uncoordinated bipy molecules interacting with both sides of the interlayer space of the host. The quantitative estimation of low-spin and high-spin iron(II) fractions in compound **2** would be important for checking the relative amount of $[Fe(bipy)_3]^{2+}$ units contained in the solid, but some of the results obtained for the material indicate that the determination of the relative amount of distinct iron sites from the ratio of the spectral areas of the corresponding subspectra [a frequent application of ^{57}Fe Mössbauer spectroscopy, often directed to the evaluation of iron(II) and iron(III) fractions] might be misleading. This problem merits further attention in the future, and is briefly exemplified by considering the data obtained for compound **6**, c-ZrP–$phen_{0.45}$–$Fe_{0.41}$, which contains both $[Fe(phen)_3]^{2+}$ and a high-spin iron(II) species. If phen is considered completely engaged in forming $[Fe(phen)_3]^{2+}$, the maximum value for the ratio of the two iron(II) species (low-spin/high-spin) should be 0.6, while a lower value is expected if the high-spin complex contains phen, as is probably the case. Surprisingly, the computer analysis of the spectra gives 1.5 as the value for the two iron(II) species ratio. For a given site, the Mössbauer resonance intensity is proportional to the number of atoms in that site times the value of the so-called recoil-free fraction, f, which, in simple terms, is related to the strength and tightness of the forces holding the probe atoms in the (solid) matrix. Thus, we are conjecturing that the above discrepancy could derive primarily from an anomalously large difference between the f values of the two iron sites.

The c-ZrP–dmp–iron systems exemplified in compounds **4**, **5** and **9** all show the partial transformation of iron into iron(III) species, as found in the a-ZrP–dmp–iron intercalates.[12] In none of the dmp compounds does the precise identification of both iron(II) and iron(III) fractions seem feasible, although, as previously discussed, d values of high-spin iron(II) species provide useful indications. It is worth noting that the spectrum of compound **4** closely resembles that published by Tomita *et al.*[13] for a dmp compound reported to have the composition c-ZrP–$dmp_{0.200}$–$Fe_{0.144}$. The presence in our case of two distinct, small (apparently), high-spin iron(II) components makes it probable that we are dealing with a similar material. At variance with Tomita *et al.*,[13] we assign the most intense component of the spectrum to a high-spin iron(III) species, accepting that the origin of the two iron(II) doublets should be dmp–Fe^{2+} complexes. Our fit gave $d = 0.93$ mm s^{-1} for one of these doublets which could be due to a five-coordinate species.

The Mössbauer results for the three crystalline c-TiP–diamine–iron compounds **11**–**13** are also reported in Table 5. In no case does the data point to the presence of an iron–trischelate species, even for compound **12** in spite of its 1:3 iron/bipy molar ratio. The small amount of iron in the c-TiP–phen material (compound **11**) is an iron(III) species. In the bipy– and dmp–iron intercalates (compounds **12** and **13**) the metal ion undergoes partial oxidation to Fe^{3+}. The spectral parameters for both iron(III) and iron(II) components suggest the presence in these materials of similar iron species; in particular, the d values measured for the high-spin Fe^{2+} site account for an FeO_6 chromophore, ruling out the occurrence of bipy or dmp coordination to iron.

Thermal behaviour and stability

The TG–DTA curves (in simultaneous mode) for most of the compounds of Table 2 are reported in Fig. 2–7. By carefully examining all the thermal curves, some general observations can be made. All the materials lose their hydration water up to 200 °C in two or more endothermic steps. The mass loss is reversible since water is rapidly regained from the surroundings. Around 300–350 °C the elimination of the organics generally begins, occurring in stages, as is indicated by a series of subsequent exothermic effects accompanying the mass losses.

The combustion is essentially complete at 700–750 °C. The loss of the diamines overlaps with condensation of the unchanged dihydrogenphosphate groups with layered pyrophosphate followed by a sharp exotherm around 950 °C related to the transition to cubic ZrP_2O_7 (confirmed by XRD). These processes also occur in the precursors[7] and in the a- and c-ZrP and a- and c-TiP pure ion exchangers.[18]

The presence of iron in the solids, whether coordinated to the ligand or not, always causes differences in the thermal behaviour with respect to the corresponding precursors. The losses of the organic ligands all go to completion at 100 °C below the temperature at which each precursor loses its own ligand, whereas each diamine behaves differently as regards the beginning of the loss. The phen elimination from compounds **1** and **6** is anticipated at about 150 °C in comparison with pure c-ZrP–$phen_{0.48}$. For compound **3**, bipy loss occurs in the range 400–750 °C, *i.e.* a much more restricted range than that of 300–970 °C for the precursor. In compounds **5** and **10**, the dmp losses begin, respectively, about 50 and 100 °C before that in c-ZrP–$dmp_{0.44}$ and end at 750 and 650 °C, whereas for the precursor, dmp is lost with a long tail up to 1000 °C. For all the exchanged materials the transition to cubic zirconium pyrophosphate occurs 50–100 °C earlier than in the parent compounds.

Interesting considerations can be made of the particular behaviour of some compounds. Fig. 2 shows the TG–DTA curves of compounds **1** and **6** and those of pure c-ZrP–$phen_{0.45}$. Phen is eliminated from compound **1** in a single step as in the precursor (see the respective DTA curves). This suggests that in both c-ZrP–$phen_{0.45}$ and c-ZrP–$phen_{0.45}$–$Fe_{0.15}$, phen is linked between the layers in a single mode, which is, however, different in the two compounds since the elimination of the amine in the compounds occurs at temperatures which differ by 120 °C from one another. For the precursor, the nitrogens of the phenanthroline interact with the dihydrogenphosphate groups;[20] for compound **1**, for which the Mössbauer results gave a clear indication of a pure low-spin trischelate $[Fe(phen)_3]^{2+}$ complex species (*i.e.* an $[FeN_6]$ moiety), both the phen nitrogens interact with Fe^{2+}. The elimination of phen at the lower temperature could be due to a catalytic effect of the presence of iron.

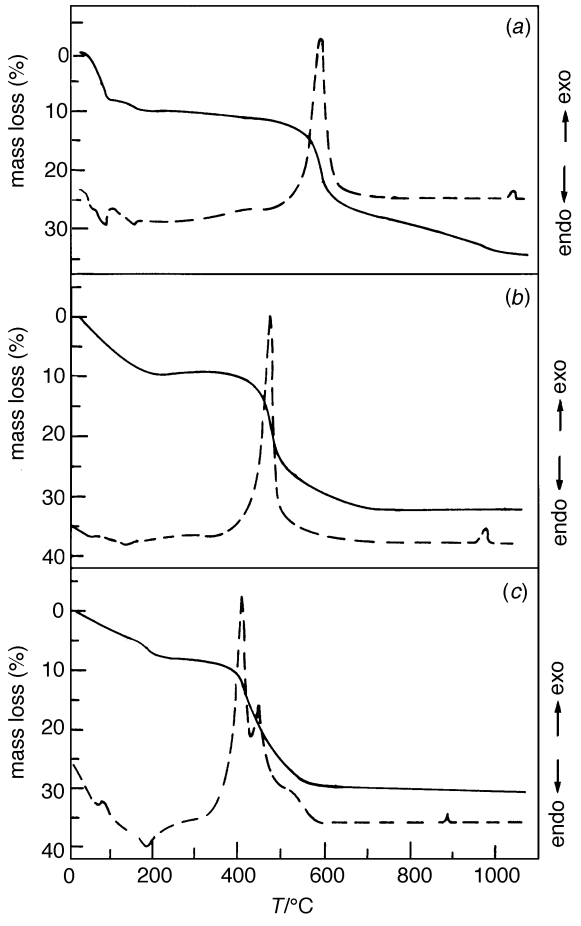

Fig. 2 Simultaneous TG–DTA curves of c-ZrP–$phen_{0.45}$ (*a*), c-ZrP–$phen_{0.45}$–$Fe_{0.15}$ (*b*) and c-ZrP–$phen_{0.45}$–$Fe_{0.41}$ (*c*)

Compound **6**, for which the Mössbauer spectra show the Fe^{2+} in both a low-spin state (able to form $[Fe(phen)_3]^{2+}$) and a high-spin state, the two exothermic effects related to the phen elimination suggest that phen is linked into two ways between the layers of c-ZrP. The part forming the trischelate is lost around 460 °C, as for compound **1**, and the other, also linked to the metal ion, but with a different, weaker bond, is lost at 410 °C.

The TG–DTA curves of compound **2** and precursor c-ZrP–$bipy_{0.27}$ are reported in Fig. 3. Compound **2** gives a large exothermic peak with a maximum at 480 °C and a shoulder on either side, the more pronounced on the right. The latter is found to correspond with the thermal effect of the precursor at 550 °C. The small shoulder on the left corresponds to the smaller distinct peak at 400 °C, of c-ZrP–$bipy_{0.27}$. Thus, the thermal effect at 480 °C can be related to the burning of the bipy linked to the low-spin Fe^{2+} in a trischelate species (see the Mössbauer results for compound **2**), whereas the two shoulders at 400 and 550 °C could be due to the elimination of a bipy linked to the host as in the precursor.

The TG–DTA curves of compounds **3** and **8**, both derived from c-ZrP–$bipy_{0.44}$, are reported in Fig. 4, together with those of the precursor for comparison. In the range 300–600 °C of the bipy loss, compound **3** shows a strong exothermic effect with a maximum at 478 °C and a small shoulder on its right side, a behaviour different from that of the precursor in which bipy has a more complicated interaction with the host (see the respective DTA curves). The Mössbauer results clearly indicate the presence of only low-spin Fe^{2+}, indicating the formation of a trischelate complex species (like compound **3**). Over the same temperature range, compound **8** shows two exothermic effects that are not clearly correlated with the Mössbauer results.

The TG–DTA curves of compounds **4** and **9** derived from

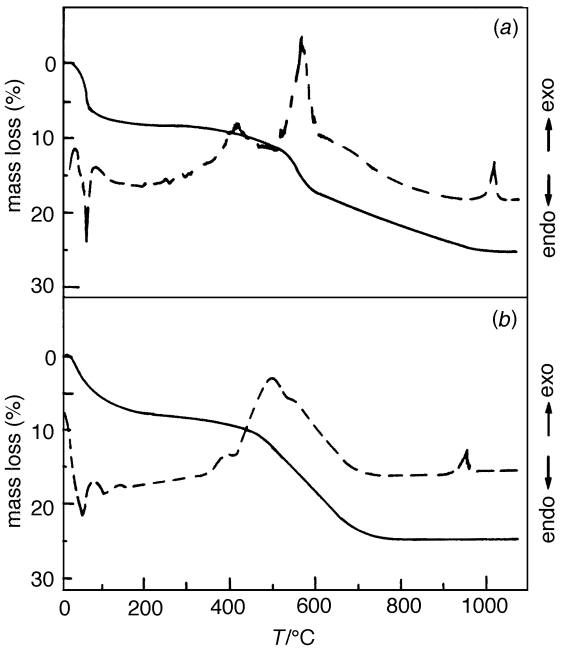

Fig. 3 Simultaneous TG–DTA curves of c-ZrP–$bipy_{0.27}$ (*a*) and c-ZrP–$bipy_{0.26}$–$Fe_{0.09}$ (*b*)

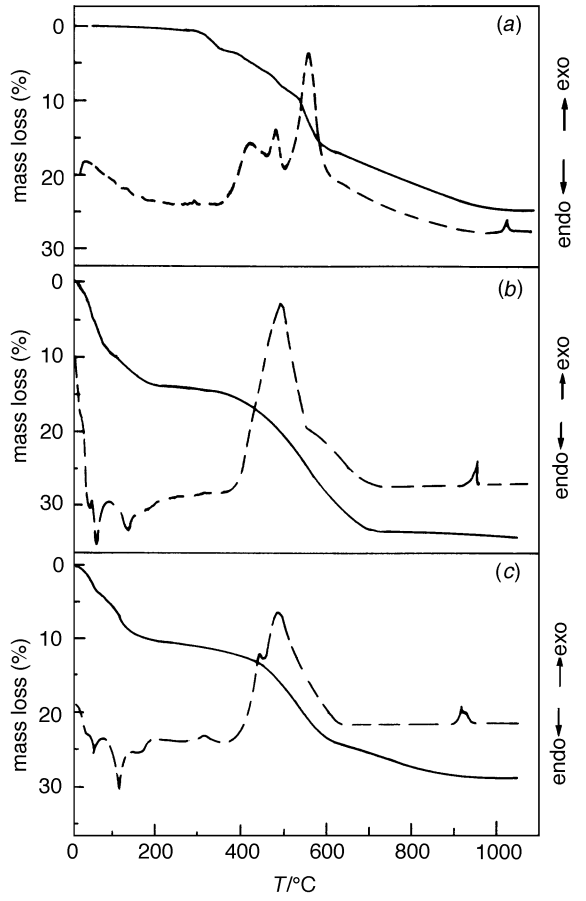

Fig. 4 Simultaneous TG–DTA curves of c-ZrP–bipy$_{0.44}$ (*a*), c-ZrP–bipy$_{0.44}$–Fe$_{0.13}$ (*b*) and c-ZrP–bipy$_{0.44}$–Fe$_{0.38}$ (*c*)

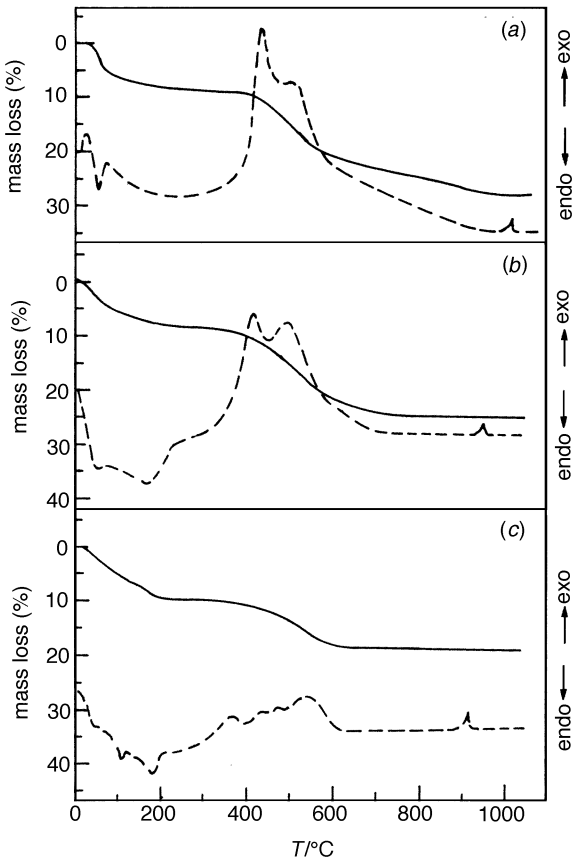

Fig. 5 Simultaneous TG–DTA curves of c-ZrP–dmp$_{0.27}$ (*a*), c-ZrP–dmp$_{0.20}$–Fe$_{0.09}$ (*b*) and c-ZrP–bipy$_{0.10}$–Fe$_{0.27}$ (*c*)

c-ZrP–dmp$_{0.27}$, are in very good agreement with the exchange data. The thermal curves are reported in Fig. 5 together with those of the precursor. Both materials suffered severe elution of diamine on Fe^{2+} uptake. For the temperature range relating to dmp elimination, compound **4**, the less eluted of the two, shows a DTA curve very similar in shape, peak position and intensity, to that of c-ZrP–dmp$_{0.27}$. This probably means that dmp is not involved in complex formation with the metal ion, so that the diamine leaves the solid at the same temperatures and with the same thermal effects as in the precursor. In compound **9**, where the amount of dmp is strongly reduced, the various, small exo- and endothermal effects occurring in the range 300–600 °C are mostly related to pyrophosphate condensation and the formation of iron–zirconium phosphate salts.

The thermal behaviour of compounds **5** and **10** derived from c-ZrP–dmp$_{0.42}$, is given in Fig. 6. It can be observed that the two DTA curves are very similar and that, compared to that of the precursor, they show a new peak around 330–340 °C that could be related to salt formation and not to pyrophosphate condensation, which usually starts around 400 °C. Furthermore, the subsequent exothermic effects, a peak with a maximum around 415 °C and a shoulder on the right side, can be nicely superimposed on those of c-ZrP–dmp$_{0.42}$. Thus, again, coordination compounds are not formed in the interlayer region of c-ZrP. Since the same behaviour was found in the a-ZrP analogue[12] it can be supposed that, in the constrained space of the interlayer region of these exchangers the dmp, with its two methyl groups in *ortho* positions to the diamine nitrogens, cannot approach the metal ion closely enough to establish coordination bonds.

The thermal behaviour of the c-TiP derivatives (compounds **11**–**14** of Table 4) is shown in Fig. 7 where the TG–DTA

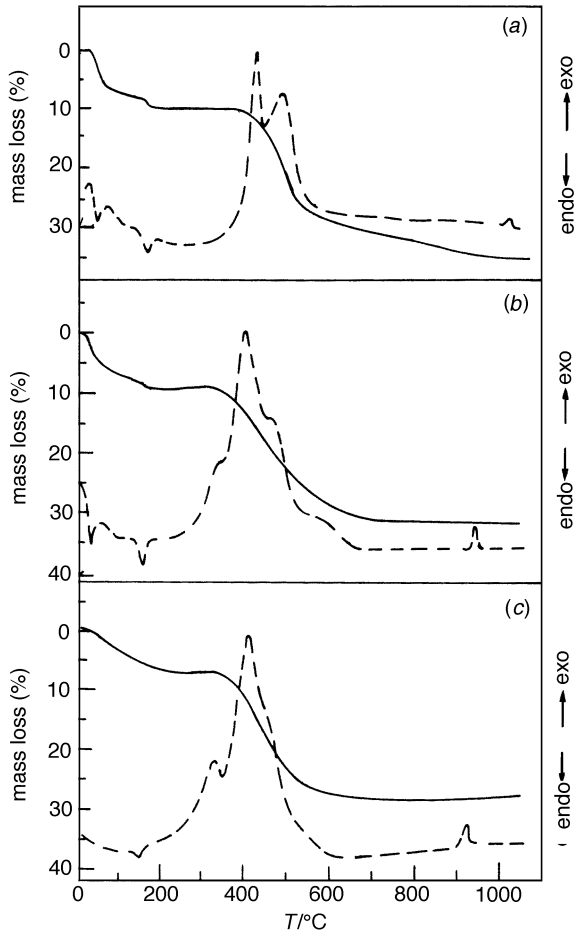

Fig. 6 Simultaneous TG–DTA curves of c-ZrP–dmp$_{0.42}$ (*a*), c-ZrP–dmp$_{0.39}$–Fe$_{0.13}$ (*b*) and c–ZrP–bipy$_{0.38}$–Fe$_{0.0.24}$ (*c*)

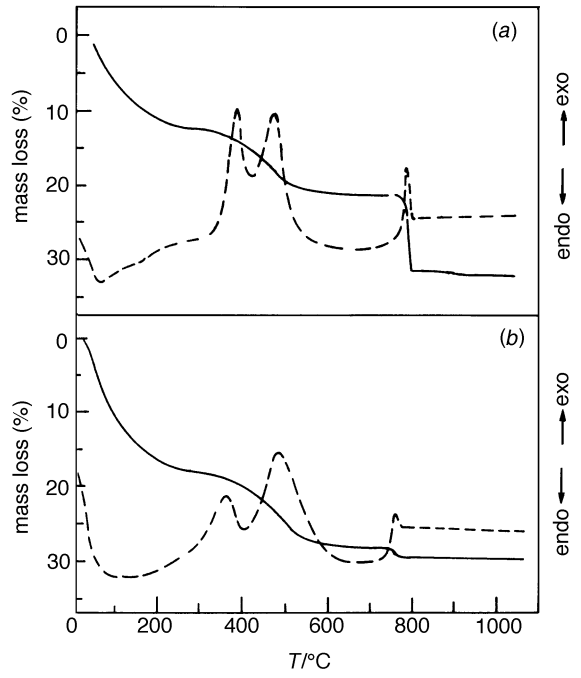

Fig. 7 Simultaneous TG–DTA curves of c-TiP–$dmp_{0.24}$ (*a*) and c-TiP–$dmp_{0.10}$–$Fe_{0.09}$ (*b*)

curves of compound **13**, c-TiP–$dmp_{0.10}$–$Fe_{0.09}$ and c-TiP–$dmp_{0.24}$ are reported. The two exothermic peaks shown by the exchanged material in the range 300–600 °C coincide with those of c-TiP–$dmp_{0.24}$, although they are somewhat enlarged. These features are probably related to the slight amorphization undergone by the solid as a consequence of the dmp partial elution. Apart from compound **14**, which contains very little dmp, the other three materials behave in the same way as their respective precursors and this is in agreement both with the fact that the compounds contain only small amounts of iron and with the Mössbauer results, which completely exclude the presence of coordinated species.

Conclusions

A series of iron(II)-exchanged materials derived from five c-ZrP–diamine (phen, bipy, dmp) intercalates has been prepared. In two cases pure Fe^{II} low-spin amine trischelates $[Fe(phen)_3]^{2+}$ and $[Fe(bipy)_3]^{2+}$ have been formed *in situ*, between the layers of the precursors c-ZrP–$phen_{0.45}$ and c-ZrP–$bipy_{0.44}$, respectively. These are important results because complex species 'constructed' in a layered material can provide a host of engineered small-pore metal-complex pillared compounds of interest in many fields, *e.g.* heterogeneous catalysis.[10,11]

Usually, the coordination chemistry in the constrained space of the interlayer region of these layered ion-exchangers is different from that found in complexes formed in solution. M^{n+}–phen or –bipy 1:1 and/or 1:2 complexes (M^{n+} = transition-metal ion) are formed in these materials,[7] which do not exist in solution. Fe^{2+} low-spin trischelates have been obtained thus far only in a-ZrP–$phen_{0.5}$, not in a-ZrP–$bipy_{0.25}$ or a-ZrP–$dmp_{0.5}$,[12] a behaviour similar to the c-ZrP–diamine derivatives. The lack of complex formation in the c-ZrP–dmp precursors is probably due to the two methyl groups in *ortho* positions to the nitrogens of dmp, a position that represents a serious hindrance to the formation of coordination compounds in the rigid interlayer region.

The c-TiP–diamine intercalates are not as reactive towards iron ions as they are, for example, to silver ions with which the same diamines form intercalation compounds which are able to perform interesting separations of transition-metal ions.[27] This confirms that the complex formation in these materials is not merely a question of space, whether restrained or not, between the layers of the materials, but also of an 'affinity' between the ligand and the metal ion to be coordinated.

The authors thank the Ministero dell'Università e della Ricerca Scientifica e Tecnologica (MURST, Roma) for financial support, and Mrs. P. Cafarelli and Mr. R. Di Rocco for technical help.

References

1 D. O'Hare, in *Inorganic Materials*, ed. D. W. Bruce and D. O'Hare, Wiley, Chichester, 1992, ch. 4.
2 *Expanded Clays and Other Microporous Solids*, ed. M. L. Occelli and H. E. Robson, Van Nostrand Reinhold, New York, 1992.
3 A. Clearfield and J. A. Stynes, *J. Inorg. Nucl. Chem.*, 1964, **26**, 117.
4 A. Clearfield, R. H. Blessing and J. A. Stynes, *J. Inorg. Nucl. Chem.*, 1968, **30**, 2249.
5 A. Clearfield and G. D. Smith, *Inorg. Chem.*, 1969, **8**, 431.
6 A. N. Christensen, E. K. Andersen, I. G. K. Andersen, G. Alberti, M. Nielsen and M. S. Lehmann, *Acta Chem. Scand.*, 1990, **44**, 865.
7 C. Ferragina, A. Frezza, A. La Ginestra, M. A. Massucci and P. Patrono, in *Expanded Clays and Other Microporous Materials*, ed. M. L. Occelli and H. E. Robson, Van Nostrand Reinhold, New York, 1992, ch. 13 and refs. therein.
8 C. Ferragina, M. A. Massucci, P. Patrono, A. La Ginestra and A. A. G. Tomlinson, *J. Chem. Soc., Dalton Trans.*, 1986, 265.
9 C. Ferragina, A. La Ginestra, M. A. Massucci, P. Patrono and P. Cafarelli, in *Ion Exchange Processes: Advances and Applications*, ed. A. Dyer, M. J. Hudson and P. A. Williams, Royal Society of Chemistry, Cambridge, 1993, pp. 345–352.
10 P. Giannoccaro, C. F. Nobile, G. Moro, A. La Ginestra, C. Ferragina, M. A. Massucci and P. Patrono, *J. Mol. Catal.*, 1989, **53**, 349.
11 P. Giannoccaro, C. Ferragina, G. Mattogno, A. La Ginestra and M. A. Massucci, *J. Mol. Catal.: A*, 1996, **111**, 135.
12 G. Alonzo, N. Bertazzi, P. Cafarelli, C. Ferragina, A. La Ginestra, M. A. Massucci and P. Patrono, *Ann. Chim. (Rome)*, 1991, **81**, 655.
13 I. Tomita, K. Sasaki, Y. Hasegawa, M. Takeda and M. Takahashi, *J. Incl. Phenom. Mol. Recognit.*, 1992, **14**, 317.
14 S. Yamanaka and M. Tanaka, *J. Inorg. Nucl. Chem.*, 1979, **41**, 45.
15 S. Allulli, C. Ferragina, A. La Ginestra, M. A. Massucci and N. Tomassini, *J. Inorg. Nucl. Chem.*, 1977, **39**, 1043.
16 C. Ferragina, M. A. Massucci and A. A. G. Tomlinson, *J. Chem. Soc., Dalton Trans.*, 1990, 1191.
17 C. Ferragina, A. La Ginestra, M. A. Massucci, P. Cafarelli, P. Patrono and A. A. G. Tomlinson, in *Recent Developments in Ion-Exchange 2*, ed. P.A. Williams and M.J. Hudson, Elsevier, New York, 1990, p. 103–108.
18 A. La Ginestra and M. A. Massucci, *Thermochim. Acta*, 1979, **32**, 241.
19 C. Ferragina, M. A. Massucci and G. Mattogno, *J. Incl. Phenom. Mol. Recognit. Chem.*, 1989, **9**, 529.
20 M. Arfelli, G. Mattogno, C. Ferragina and M. A. Massucci, *J. Incl. Phenom. Mol. Recognit. Chem.*, 1991, **11**, 15.
21 C. Ferragina, M. A. Massucci, A. La Ginestra, P. Patrono and A. A. G. Tomlinson, *J. Chem. Phys.*, 1985, **89**, 4762.
22 C. Ferragina, M. A. Massucci and A. A. G. Tomlinson, *J. Chem. Soc., Dalton Trans.*, 1990, 1191.
23 C. Ferragina, M. A. Massucci, A. La Ginestra, P. Patrono and A. A. G. Tomlinson, *J. Chem. Soc., Dalton Trans.*, 1986, 265; 1988, 851.
24 C. Ferragina, P. Cafarelli, R. Di Rocco and M. A. Massucci, *Thermochim. Acta*, 1995, **269/270**, 507.
25 C. Ferragina, A. La Ginestra, M. A. Massucci, G. Mattogno, P. Patrono, P. Giannoccaro, P. Cafarelli and M. Arfelli, *J. Mater. Chem.*, 1995, **5**, 461.
26 C. Ferragina, M. A. Massucci, P. Patrono, A. A. G. Tomlinsom and A. La Ginestra, *Mater. Res. Bull.*, 1987, **22**, 29.
27 C. Ferragina, M. A. Massucci and A. A. G. Tomlinson, *J. Mater. Chem.*, 1996, **6**, 645.
28 I. Dezsi and L. Keszthelyi, *Solid State Commun.*, 1966, **4**, 511.
29 B. Brunot, *Chem. Phys. Lett.*, 1974, **29**, 368.
30 B. Brunot, *Chem. Phys. Lett.*, 1974, **29**, 371.
31 W. M. Reiff, R. B. Frankel and C. R. Abeledo, *Chem. Phys. Lett.*, 1974, **22**, 368.

Paper 6/03543D; *Received* 21*st May*, 1996